# 5 Variability and Noise in Subexcitable Nets of FitzHugh-Nagumo Elements

Spatiotemporal pattern formation in excitable and subexcitable media has been investigated since many years. Already in 1995 Jung and Mayer-Kress studied the emergence of waves in an excitable cellular-automata-like system under the influence of additive white noise [7]. The existence of noise sustained waves has been confirmed experimentally in slices of hippocampal astrocytes [3]. Further studies on pattern formation in subexcitable media under the influence of additive noise have been performed, e.g. in the Barkley system [8]. Similar to the effect of coherence resonance [9] one gets the most coherent system response (patterns) for an intermediate noise strength. This pattern formation is a stochastic resonance effect, known as spatiotemporal stochastic resonance (STSR). Noise induced pattern formation is also studied, theoretically and experimentally, in presence of multiplicative noise instead of additive noise [62, 63].

Variability may influence the spatiotemporal dynamics of many spatially extended systems [18, 19, 20] and can play an important role for pattern formation in nets of biochemical oscillators [22, 40]. Furthermore variability may have a systematic effect, which can induce transitions between different dynamical regimes [38]. Recently it was demonstrated that variability can cause resonance-like phenomena in networks of nonlinear elements [23, 24]. A first study of the interplay of additive noise and additive variability in one dimensional chains of exitable elements was performed in [64].

Throughout this chapter subexcitable nets of FitzHugh-Nagumo elements [Eqs. (3.1)] with diffusive coupling [Eq. (2.18)] are considered, where parameter set 2 [Eq. (2.12)] is used [39, 65]. The corresponding stability analysis for a single FitzHugh-Nagumo element in dependency on the parameters $e$ and $c$ is presented in Fig. 2.5(b). The mean values $\mathfrak{E}$ and $C$ of the probability distributions from Eqs. (3.2) are chosen to be

$$(\mathfrak{E}, C) = (-0.3, 4.0). \tag{5.1}$$

Without variability each FHN element has the same parameter values $e_{ij} = \mathfrak{E}$ and $c_{ij} = C$. For the chosen parameter values and without variability each FHN element is in the excitable regime $E$, resulting in a spatially homogeneous temporally constant solution for all initial conditions [Fig. 2.15(d)]. Waves are not sustained in the absence of the stochastic terms and thus the net is in the subexcitable regime $E_S$.

## 5.1 Additive Variability and Additive Noise

Throughout this section the multiplicative noise and the multiplicative variability are neglected, while the strength of the additive variability $\sigma_{v,e}$ and the strength of the additive noise $\sigma_{n,e}$ are varied. The additive variability is considered to be white in space [Eqs. (3.3)]. The side length of the net is chosen to be $N = 256$ and the coupling strength is $q = 20$. Introducing the additive variability in the net the parameter values $e_{ij}$ change

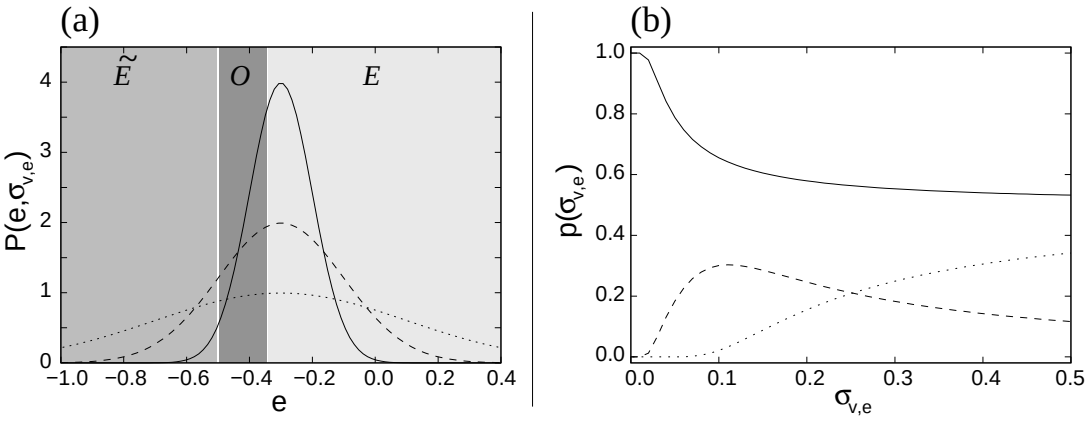


Figure 5.1. (a): The Gaussian probability distribution $P(e, \sigma_{v,e})$ for three different values of the variability strength, (—) $\sigma_{v,e} = 0.1$, (- -) $\sigma_{v,e} = 0.2$ and (· ·) $\sigma_{v,e} = 0.4$. The grey areas mark the dynamical regimes. (b): Probability $p(\sigma_{v,e})$ for one FitzHugh-Nagumo element to be in the excitable regime $E$ (—), the oscillatory regime $O$ (- -) and the excitable regime $\tilde{E}$ (· ·) in dependency on the variability strength $\sigma_{v,e}$.

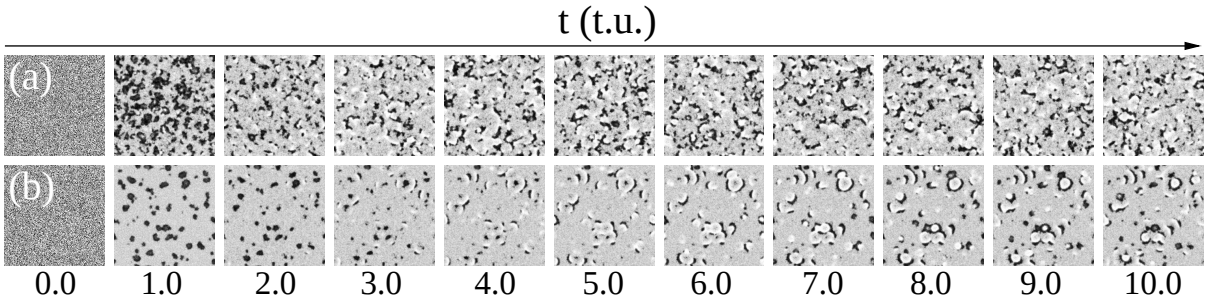


Figure 5.2. Snapshots of $u_{ij}(t)$ for a net of FHN elements [Eqs. (3.1)] with diffusive coupling [Eq. (2.18)] in dependency on the integration time $t$ for random initial conditions, $q = 20$ and $N = 256$. (a): Noise induced pattern formation for $\sigma_{n,e} = 0.1$ and $\sigma_{v,e} = 0$. (b): Variability induced pattern formation for $\sigma_{v,e} = 0.15$ and $\sigma_{n,e} = 0$.

from element to element. A change in this parameter shifts the linear nullcline of the FHN elements [Fig. 2.6(b)], which has a strong influence on their dynamics [Fig. 5.1(a)]. A subexcitable net of FHN elements with variability in parameter $e$ thus consists of elements in different dynamical regimes. For $e_{ij} > -0.337$ the single element has a stable focus and its dynamics is excitable. For the parameter range $-0.345 > e_{ij} > -0.503$ the element is in the oscillatory regime $O$. For even smaller values of the parameter $e$ the element becomes excitable again, but the stable focus is now at the upper stable branch of the cubic nullcline. The element is in the regime $\tilde{E}1$. Between the excitable regimes and the oscillatory regime small areas in parameter space exist, where a stable focus and a stable limit cycle coexist [white bands in Fig. 5.1(a)]. These additional regimes, $O3$ and $\tilde{O}3$, are not important for the investigations presented in this chapter and can be neglected. The probability for an element to be in a certain regime depends on $\sigma_{v,e}$, what is shown in Fig. 5.1(b).

For a weak noise strength the probability of an element to get excited by the noise is almost zero and no pattern formation can be observed. This behaviour changes abruptly, if

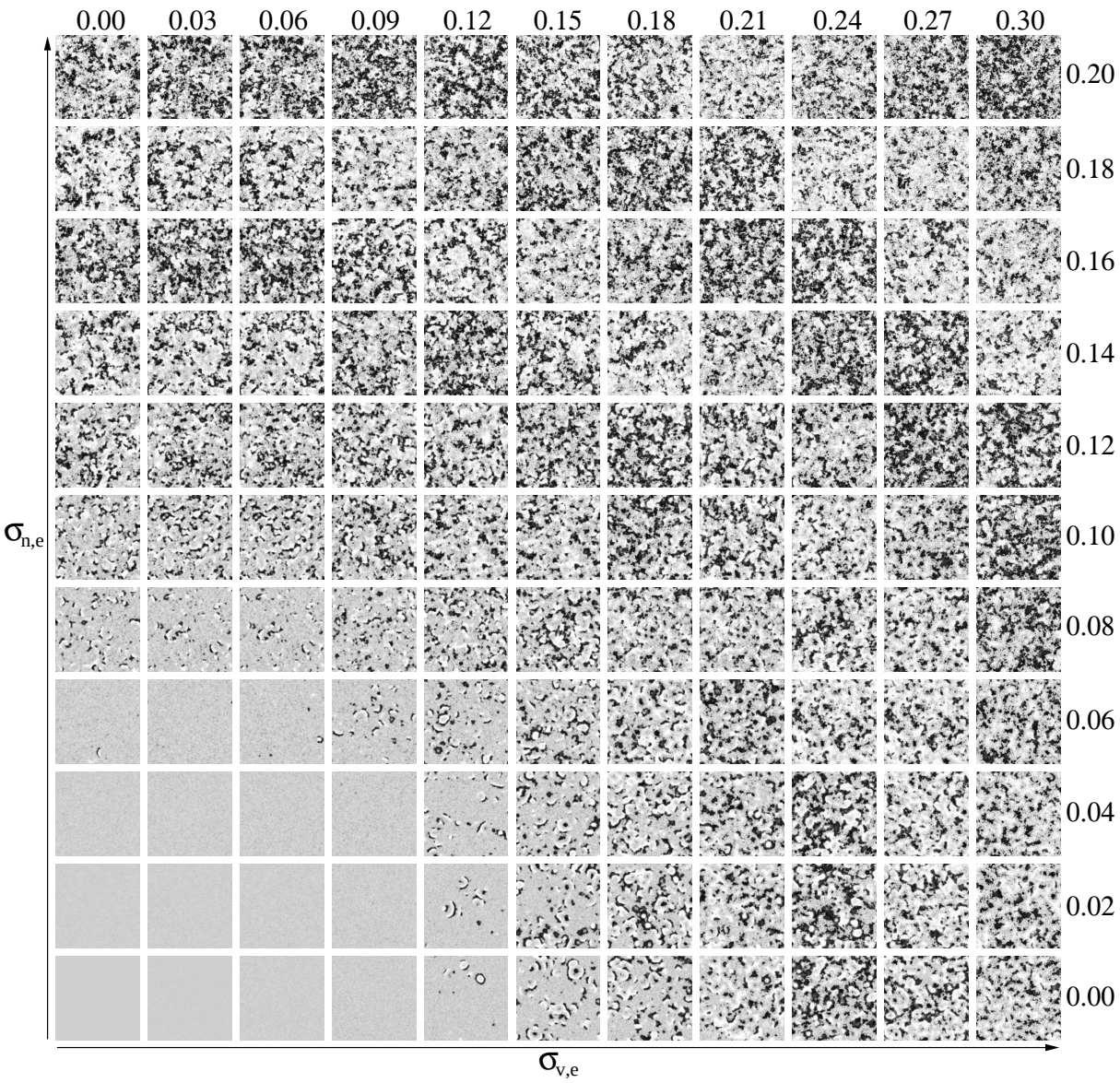


Figure 5.3. Snapshots of $u_{ij}(t)$ for a net of FHN elements [Eqs. (3.1)] with diffusive coupling [Eq. (2.18)] in dependency on the variability strength $\sigma_{v,e}$ and the noise strength $\sigma_{n,e}$ for $t = 40$ $t.u.$, random initial conditions, $q = 20$ and $N = 256$.

a certain threshold of the noise strength is reached. Now there is a much higher probability for each element in the medium to become excited. These excitations spread out in the net and pattern formation can be observed [Fig. 5.2(a)]. The most coherent patterns are found for intermediate noise strengths. For large noise strengths the coherent patterns are destroyed. This dependency on the noise strength, which is called spatiotemporal stochastic resonance (STSR), is visible in the first column of Fig. 5.3.

If the additive noise is replaced by variability in parameter $e$ one has instead of a stochastic external forcing a heterogeneous net. For small variability strengths $\sigma_{v,e} < 0.12$ no pattern formation can be observed, whereas for a slightly larger variability strength one observes the development of wave fronts in the subexcitable net [Fig. 5.2(b)]. A further increase of the variability strength leads to a destruction of the coherent structures, what is exhibited in the lowest row of Fig. 5.3.

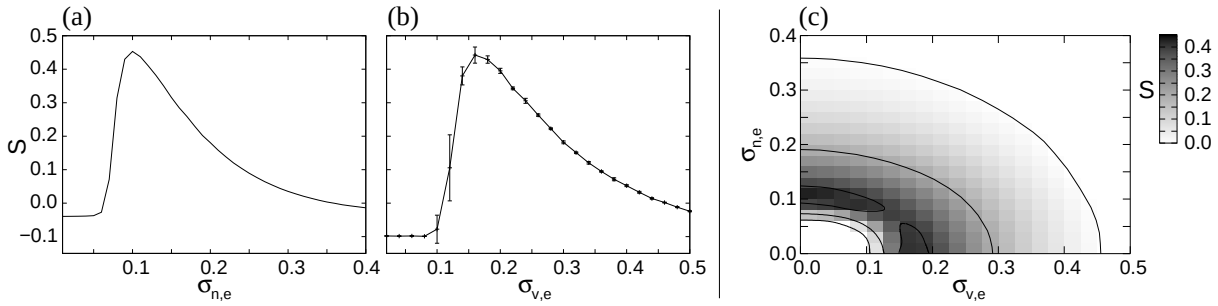


Figure 5.4. The cross correlation $S$ [Eq. (2.24)] for a net of FitzHugh-Nagumo elements [Eqs. (3.1)] with diffusive coupling [Eq. (2.18)], averaged over ten realisations of the net for $q = 20$ and $N = 256$, (—) $S = 0.4$, 0.2 and 0.0. (a): In dependency on the noise strength $\sigma_{n,e}$ for $\sigma_{v,e} = 0$. (b): In dependency on the variability strength $\sigma_{v,e}$ for $\sigma_{n,e} = 0$. (c): In dependency on the variability strength $\sigma_{v,e}$ and the noise strength $\sigma_{n,e}$.

At the first view this phenomenon looks similar to STSR induced by additive white noise, but the development of the patterns is different and so are the observed structures. In the case of noise induced STSR the stochastic external driver randomly excites elements in the net. The excited elements act as excitation centres, from which the waves spread through the medium. The excitation centres are not fixed and thus the patterns change their shape strongly in time [Fig. 5.2(a)]. In the case without noise but with additive variability one increases the diversity between the elements in the net with growing $\sigma_{v,e}$. For $\sigma_{v,e} < 0.03$ nearly all elements are excitable [Fig. 5.1(b)]. This changes for larger variability strengths, where a reasonable amount of elements becomes oscillatory. However, due to the spatial coupling, these elements do not show oscillatory dynamics for $\sigma_{v,e} \lesssim 0.12$ and the spatiotemporally homogeneous solution of the net stays stable. Further increasing the variability strength the diversity in the net is large enough to destroy the spatially homogeneous temporally constant net dynamics. Single elements or small clusters of elements start to oscillate. These oscillating elements act now as fixed excitation centres, from which the waves spread through the subexcitable net. The deterministic heterogeneous net thus generates periodic excitation waves. After a short transient time the excitation patterns are recurrent with an oscillation period of approximately $1t.u.$ [Fig. 5.2(b)]. If the additive variability strength is further increased the coupling is not able to conserve an ordered net dynamics anymore and the dynamics of the single elements becomes more and more dominant. The coherent structures are destroyed.

Applying the spatial cross correlation $S$ [Eq. (2.24)], which is displayed in Fig. 5.4 in dependency on the noise strength $\sigma_{n,e}$ and the variability strength $\sigma_{v,e}$, one can measure the coherence of the observed patterns. In Fig. 5.4(a) one clearly sees that the coherence of the noise induced patterns shows a resonance-like behaviour in dependency on the noise strength for $\sigma_{v,e} = 0$, what is a well known result [8]. More interesting is the case of an increasing variability strength $\sigma_{v,e}$ for a net without noise, which is plotted in Fig. 5.4(b). One again sees a distinct resonance curve with a maximum at $\sigma_{v,e} \approx 0.15$. This proofs that the variability induced pattern formation is, similar to the noise induced STSR, a resonance-like effect.

Now the interplay of additive variability and additive noise is studied. In Fig. 5.3 snapshots of the fast variable of a net of FHN elements are displayed for different values of $\sigma_{n,e}$ and $\sigma_{v,e}$. One clearly sees that the variability strength, for which the pattern formation

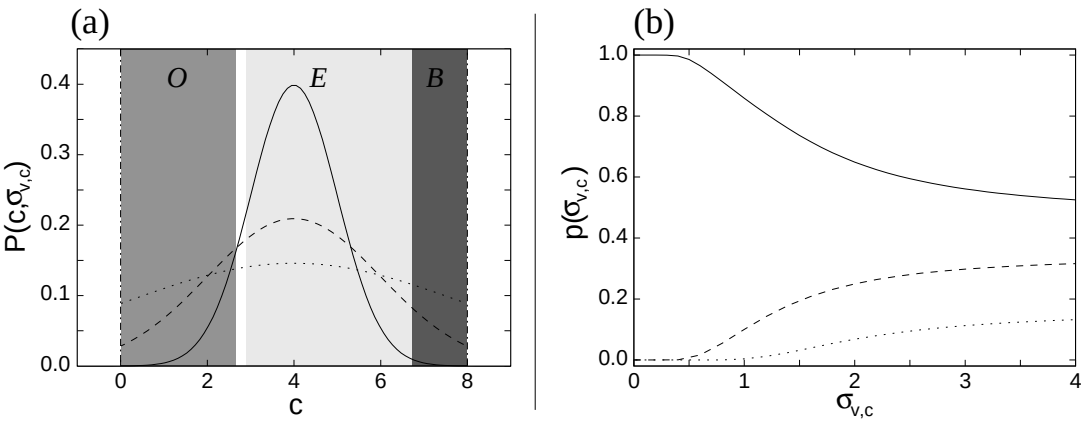


Figure 5.5. (a): The Gaussian probability distribution $P(c, \sigma_{v,c})$ for three different values of the variability strength, (—) $\sigma_{v,c} = 1$, (- -) $\sigma_{v,c} = 2$ and (· ·) $\sigma_{v,c} = 4$. (· - ·) cut-off of the probability distribution. The grey areas mark the dynamical regimes. (b): Probability $p(\sigma_{v,c})$ for one FitzHugh-Nagumo element to be in the excitable regime $E$ (—), the oscillatory regime $O$ (- -) and the bistable regime $B$ (· ·) in dependency on the variability strength $\sigma_{v,c}$.

sets in, decreases with growing noise strength $\sigma_{n,e}$ and vice versa. This behaviour leads to an elliptical symmetry concerning the onset of pattern formation. This symmetry is confirmed by the cross correlation $S$ plotted in Fig. 5.4(c), which as a whole shows an elliptical symmetry. The ridge (maximum) of $S$ marks the values of $\sigma_{v,e}$ and/or $\sigma_{n,e}$, for which the most coherent patterns are found. Following this line the pattern formation shows a continuous transition from periodic excitation waves for $\sigma_{n,e} = 0$ to noise induced STSR for $\sigma_{v,e} = 0$. The pattern formation mechanism is obviously different for noise and variability, but the structures at a fixed time look similar.

Studying the influence of the coupling strength one finds that a minimum value $q \approx 5$ is needed to observe a coherent net dynamics. For larger values of the coupling strength a further increase of $q$ has no strong influence on the variability and/or noise induced pattern formation presented in this section. The pattern formation, and thus the resonance curve, is just shifted to larger values of $\sigma_{v,e}$ and $\sigma_{n,e}$, respectively.

## 5.2 Multiplicative Variability and Multiplicative Noise

Throughout this section the influence of multiplicative noise and multiplicative variability is studied, while additive variability and additive noise are neglected. The multiplicative variability is considered to be white in space, where the correlation function is given by Eqs. (3.5). The side length of the net is chosen to be $N = 256$ and the coupling strength $q$ is varied. Introducing the multiplicative variability in the net the parameter values $c_{ij}$ change from element to element and the net is again a mixture of elements in different dynamical regimes [Fig. 2.5(b) and Fig. 5.5(a)]. For $c_{ij} < 2.66$ the single element is in the oscillatory regime $O$, for $2.91 < c_{ij} < 6.71$ the element is excitable ($E$) and for $c_{ij} > 6.71$ the element is in the bistable regime $B$. Between the excitable regimes and the oscillatory regime a small area in parameter space exist, where a stable focus and a stable limit cycle coexist [white band in Fig. 5.5(a)]. This additional regime $O3$ is not important for the investigations presented in this section and can be neglected. The probability

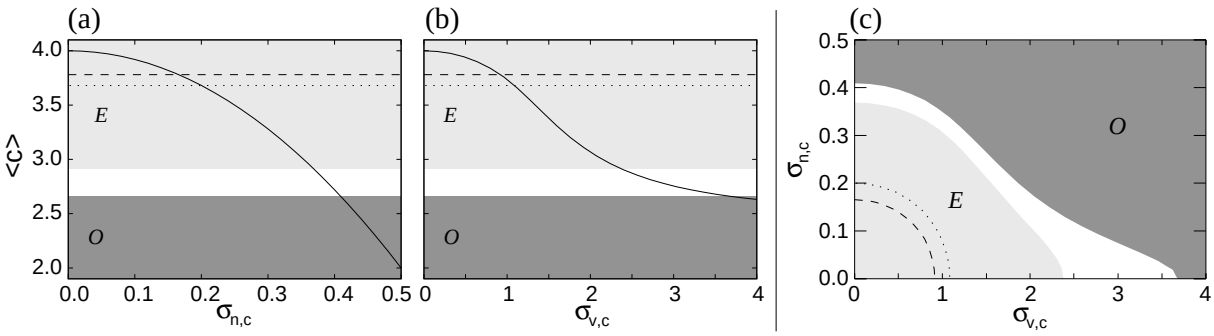


Figure 5.6. Effective mean value $\langle c \rangle$ [Eq. (3.10)] for nets of FHN elements [Eqs. (3.1)], expected transition to an subexcitable net (· ·) for $q = 10$ and (- -) for $q = 20$. The grey areas mark the dynamical regimes. (a): In dependency on the noise strength $\sigma_{n,c}$ for $\sigma_{v,c} = 0$. (b): In dependency on the variability strength $\sigma_{v,c}$ for $\sigma_{n,c} = 0$. (c): In dependency on the noise strength $\sigma_{n,c}$ and the variability strength $\sigma_{v,c}$.

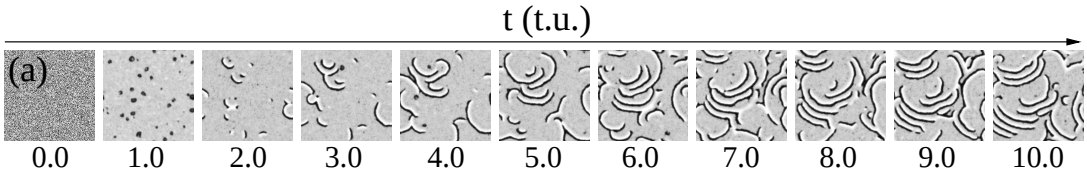


Figure 5.7. Snapshots of $u_{ij}(t)$ for a net of FHN elements [Eqs. (3.1)] with diffusive coupling [Eq. (2.18)] in dependency on the integration time $t$ for random initial conditions, $q = 20$, $N = 256$ and $\sigma_{v,c} = 0$. Pattern formation induced by multiplicative noise for $\sigma_{n,c} = 0.3$ (regime $E_P$).

for an element to be in a certain regime depends on $\sigma_{v,c}$ [Fig. 5.1(b)]. The probability distribution $P(c, \sigma_{v,c})$ is, as explained in Section 4.2, set to zero for $c < 0$ and $c > 2C$ [cut-off in Fig. 5.5(a)].

The multiplicative variability in parameter $c$ has, in difference to additive variability, a systematic influence on the net dynamics, which changes the global net parameter $\langle c \rangle$ [Eq. (3.10)]. This parameter is also systematically influenced by the multiplicative noise, as pictured in Fig. 5.6(a). Increasing the noise strength $\sigma_{n,c}$ the effective parameter is decreasing and a transition from subexcitable to excitable net dynamics is predicted for $\sigma_{n,c} \approx 0.2$. This transition depends on the coupling strength. For noise strengths larger than $\sigma_{n,c} > 0.41$ the effective parameter $\langle c \rangle$ predicts a transition to oscillatory net dynamics. Increasing the variability strength $\sigma_{v,c}$ instead of the noise strength one finds a similar behaviour [Fig. 5.6(b)], where the transition to excitable dynamics is expected for $\sigma_{v,c} \approx 1$. Comparing Fig. 5.6(a) with Fig. 5.6(b) one discerns a clear difference. In the case of multiplicative variability the slope of $\langle c \rangle$ is decreasing for large variability strengths, a behaviour, which cannot be found for the multiplicative noise. This difference is due to the cut-off of the probability distribution $P(c, \sigma_{v,c})$ [Fig. 5.5(a)].

In Fig. 5.6(c) the combined systematic influence of the multiplicative stochastic terms on the effective parameter $\langle c \rangle$ is plotted. The transitions between the different regimes depend now on both, the strength of the multiplicative noise and the strength of the multiplicative variability. For intermediate values of $\sigma_{v,c}$ and/or $\sigma_{n,c}$ one expects excitable and for large values oscillatory dynamics.

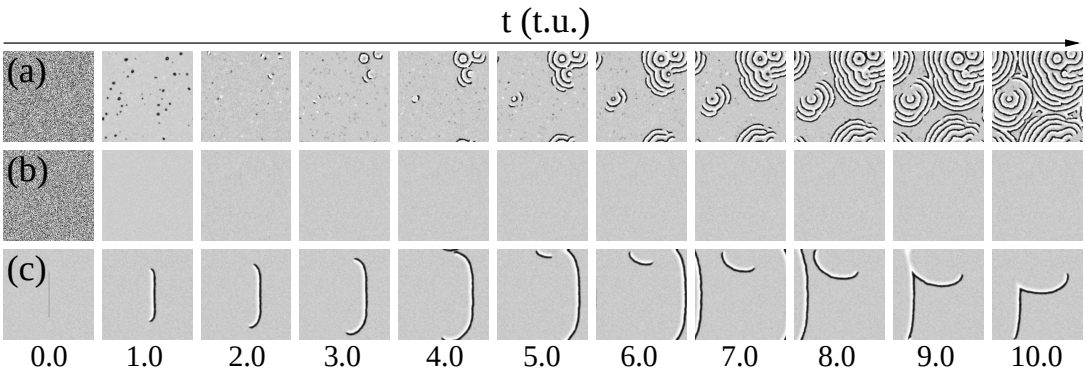


Figure 5.8. Snapshots of $u_{ij}(t)$ for a net of FHN elements [Eqs. (3.1)] with diffusive coupling [Eq. (2.18)] in dependency on the integration time $t$ for $N = 256$ and $\sigma_{n,c} = 0$. (a): Variability induced pattern formation (regime $E_P$) for random initial conditions, $q = 10$ and $\sigma_{v,c} = 4$. (b): The regime $E_H$ for random initial conditions, $q = 20$ and $\sigma_{v,c} = 2$. (c): Special initial conditions induce spiral waves for $q = 20$ and $\sigma_{v,c} = 2$.

At first a subexcitable net is investigated with multiplicative noise only. For large coupling strengths the expected transition from subexcitable to excitable net dynamics can be observed at the predicted value of $\sigma_{n,c}$. The multiplicative noise does furthermore induce wave fronts, which can, as displayed in Fig. 5.7, propagate through the whole net, if the noise strength is large enough. In this case the net is in the regime $E_P$ (see Section 4.2). For noise strengths $\sigma_{n,c} > 0.4$ one finds a more or less disturbed global oscillation, what indicates that the net is in the oscillatory regime $O$. Clear transitions to the regimes $E_P$ and $O$ are only observed for coupling strengths larger than $q \approx 5$. A further increase of the coupling strength leads to larger and broader patterns in the regime $E_P$.

The numerical integration of nets with multiplicative variability but without noise reveal a more complex net dynamics as one would expect from the prediction using the global net parameter $\langle c \rangle$. Snapshots of a net of FHN elements for different values of $q$ and $\sigma_{v,c}$ are presented in Fig. 5.8. For a coupling strength $q \lesssim 5$ the coupling is to weak to enforce a coherent net dynamics and the dynamics of the single elements dominate. The corresponding region of undefined dynamical regimes is displayed in Fig. 5.9. For larger coupling strengths, approximately $5 < q < 12$, one finds the regime $E_P$ for large variability strengths [$\sigma_{v,c} \gtrsim 2.8$ in Fig. 5.8(a)]. The net is excitable, but the homogeneous solution is not stable. Some elements or clusters of elements oscillate and induce excitations waves, which spread through the whole net. These variability induced patterns in the deterministic net are periodic in time. For even larger coupling strengths the homogeneous solution becomes stable for all values of the variability strength and for large enough $\sigma_{v,c}$ spiral waves, which propagate through the whole net, can be induced by special initial conditions [Fig. 5.8(b) and (c)]. For this part of the parameter space the excitable regime $E_H$ is realised. This is a big differences to the case of the multiplicative noise, where the regime $E_H$ is not found for corresponding parameter values.

The borders of the dynamical regimes of the net are displayed in Fig. 5.9 in dependency on the coupling strength $q$ and the variability strength $\sigma_{v,c}$. One clearly discerns all the regimes described in the previous paragraph. The regime $E_H$ is found in a large part of the parameter space and for coupling strengths $q \gtrsim 15$ the transition from $E_S$ to this excitable regime can be predicted quite well using the effective parameter $\langle c \rangle$ [Eq. (3.10)]. This again

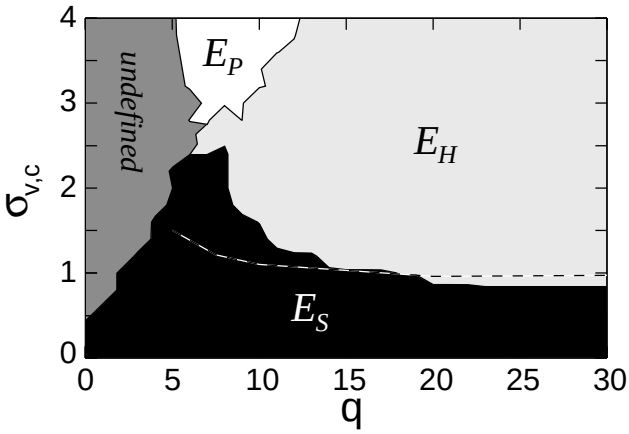


Figure 5.9. The pattern forming regimes of a net of FHN elements [Eqs. (3.1)] with diffusive coupling [Eq. (2.18)] in dependency on the coupling strength $q$ and the variability strength $\sigma_{v,c}$. Numerical results for $N = 256$ and $\sigma_{n,c} = 0$. (- -) prediction for the transition from $E_S$ to $E_H$ [Eq. (3.10)].

shows that this parameter determines the dynamical regime of a large diverse net with a strong coupling, though it can not predict, if the diverse net exhibits pattern formation or not. From Fig. 5.6 one would also expect a transition to oscillatory net dynamics for $\sigma_{v,c} \gtrsim 3.5$. This transition cannot be found, even if the variability and the coupling strength are further increased. This result reveals that for high variability strengths with broad probability distributions the approximate prediction of the net dynamics using the mean gradient angle [Eq. (3.10)] is not very precise anymore.

The multiplicative variability obviously has a completely different influence on the net dynamics than the additive variability studied in Section 5.1. For a high enough coupling strength the multiplicative variability causes a transition to the excitable net dynamics without inducing pattern formation and the regime $E_H$ is realised. Increasing $\sigma_{v,c}$ the homogeneous solution of the net stays stable and thus the observed dynamics of the net does not change. Nevertheless the multiplicative variability strongly improves the ability of the net to support excitation waves, induced for example by special initial conditions. In the following section the fixed coupling strength $q = 20$, representing the large area of parameter space, where the multiplicative variability does not induce pattern formation, is chosen to study the interplay of additive and multiplicative variability.

## 5.3 Interplay of Additive and Multiplicative Variability

In this section the interplay of white additive and white multiplicative variability is studied in a subexcitable net of FHN elements [Eqs. (3.1)]. This means that the parameter values $e_{ij}$ and $c_{ij}$ vary from element to element. The net, which is a mixture of elements in different dynamical regimes, is considered to be strictly deterministic ($\sigma_{n,e} = 0$ and $\sigma_{n,c} = 0$). A single element of the net can be in the regime $E$, $\tilde{E}$, $O$ or $B$ [Figs. 5.1 and 5.5]. The side length of the net is chosen to be $N = 256$ and the coupling strength is considered to be $q = 20$.

Simulation results for such a subexcitable net are displayed in Fig. 5.10. One discerns that increasing $\sigma_{v,e}$ leads to pattern formation for all values of $\sigma_{v,c}$. The additive variability

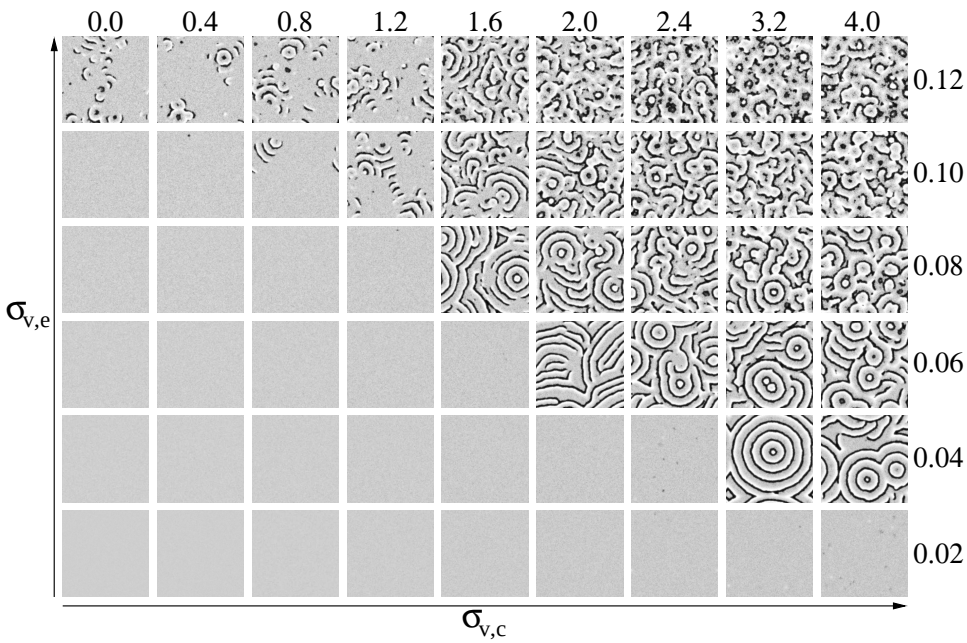


Figure 5.10. Snapshots of $u_{ij}(t)$ for a net of FHN elements [Eqs. (3.1)] with diffusive coupling [Eq. (2.18)] in dependency on the variability strengths $\sigma_{v,e}$ and $\sigma_{v,c}$ for random initial conditions, $t = 40$ $t.u.$, $q = 20$ and $N = 256$.

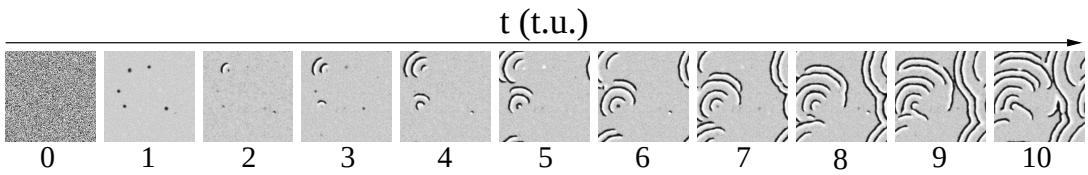


Figure 5.11. Snapshots of $u_{ij}(t)$ for a net of FHN elements [Eqs. (3.1)] with diffusive coupling [Eq. (2.18)] in dependency on the integration time $t$ for random initial conditions, $\sigma_{v,c} = 2$, $\sigma_{v,e} = 0.06$, $q = 20$ and $N = 256$.

allows the net to generate excitation waves. The multiplicative variability controls the extent and the coherence of the patterns via improving the ability of the net to support such excitation waves with increasing $\sigma_{v,c}$. For $\sigma_{v,c} \gtrsim 1.2$ increasing $\sigma_{v,e}$ leads to a transition from $E_H$ to $E_P$ and the induced excitation waves spread through the whole net. Once in the range of the additive variability strength, for which maximally coherent pattern formation is found, a further increase of $\sigma_{v,e}$ leads to the destruction of the coherent patterns. An other phenomenon observed for increasing $\sigma_{v,c}$ is the decrease of the minimal variability strength $\sigma_{v,e}$, which is required to generate excitation waves. Without multiplicative variability a variability strength $\sigma_{v,e} \approx 0.12$ is necessary to induce pattern formation, whereas for $\sigma_{v,c} > 2$ the patterns emerge already for $\sigma_{v,e} \approx 0.05$.

The pattern formation in the regime $E_P$ is displayed in detail in Fig. 5.11 for $\sigma_{v,c} = 2$ and $\sigma_{v,e} = 0.06$. In this case the additive variability is strong enough that the spatially homogeneous solution of the net is destroyed. Some elements start to oscillate and act as fixed excitation centres. Starting from these centres the waves spread through the whole net, because for the variability strength $\sigma_{v,c} = 2$ the net is excitable. After a transient the patterns are periodic in time.

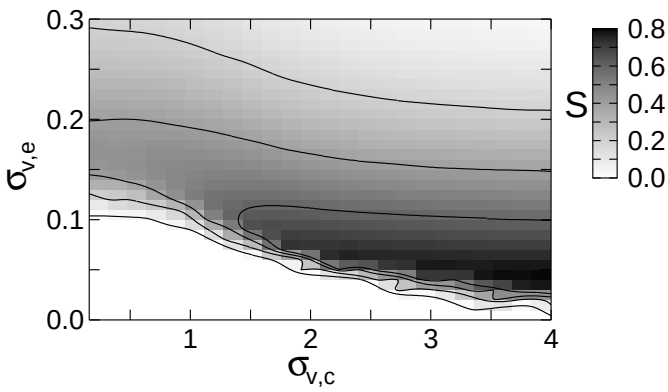


Figure 5.12. The cross correlation $S$ [Eq. (2.24)] for a net of FHN elements [Eqs. (3.1)] with diffusive coupling [Eq. (2.18)] in dependency on the variability strengths $\sigma_{v,c}$ and $\sigma_{v,e}$ averaged over ten realisations of the net for $q = 20$ and $N = 256$, (—) $S = 0.6$, 0.4, 0.2 and 0.0.

The results presented in this section are substantiated using the spatial cross correlation $S$, a measure for the coherence of the patterns, which is plotted in Fig. 5.12. One clearly discerns an increase of the maximum value of $S$ increasing the variability strength $\sigma_{v,c}$. Furthermore, increasing the variability strength $\sigma_{v,e}$ starting from $\sigma_{v,e} = 0$ for a fixed value of $\sigma_{v,c}$, the spatial cross correlation always shows a resonance-like behaviour. A larger value of $\sigma_{v,c}$ leads thereby to a displacement of the resonance curve to smaller values of the strength of the additive variability. The onset of pattern formation and also the most coherent structures are found for smaller values of $\sigma_{v,e}$.

The coherent pattern formation, induced by the interplay of the additive and the multiplicative variability, are found for a wide range of the coupling strength.

## 5.4 Summary and Conclusions

It is shown that additive variability can induce pattern formation in subexcitable nets of FHN elements. The patterns are most coherent for intermediate variability strengths. This phenomenon can be called variability induced STSR. It was furthermore demonstrated that the additive variability strongly influences the response of the net to additive noise. For a low variability strength the resonance curve regarding the additive noise strength is shifted to lower values of $\sigma_{n,e}$ increasing $\sigma_{v,e}$. The variability determines, for which value of the noise strength one finds the maximum of the resonance curve. For $\sigma_{v,e} > 0.175$ one finds a monoton decrease of $S$ for an increase of $\sigma_{n,e}$ and thus the STSR effect is destroyed.

The impact of the multiplicative variability on the net dynamics is very different compared to the one of the additive variability. In a large range of the coupling strength the multiplicative variability does not induce pattern formation, but it nevertheless has a systematic influence on the net. This systematic influence causes a transition from the subexcitable regime $E_S$ to the excitable regime $E_H$ for coupling strengths $q \gtrsim 12$ (variability induced transition). For corresponding coupling strengths the effective net parameter $\langle c \rangle$ determines the net dynamics for not to large $\sigma_{v,c}$ and predicts the reported transition quite accurate. Furthermore it is shown that the influence of multiplicative noise and multiplicative variability on the net dynamics may not always be the same.

Both induce a transition to excitable dynamics in the presented case, but in addition the multiplicative noise induces pattern formation.

Using a fixed coupling strength $q = 20$ the net itself can show coherent pattern formation in the presence of additive and multiplicative variability. For certain variability strengths one observes periodic excitation waves, which spread through the whole net. The waves are induced by the additive variability, and the ability of the net to support this waves is generated by the multiplicative variability. This means that the interplay of additive and multiplicative variability allows a complex deterministic net dynamics, where the pattern formation can neither be explained by the dynamics of the single elements of the net nor by the mean values of the model parameters. This is an interesting form of self-organisation of the net.

These results demonstrate that the interplay of additive noise and additive variability may play an important role in excitable and subexcitable biophysical systems. Variability could be essential for pattern formation mechanisms or stochastic resonance effects. At least it may influence noise induced effects, such as temporal or spatiotemporal stochastic resonance.

Multiplicative variability has in addition a systematic influence on the net dynamics, which could cause a wide range of interesting phenomena, like variability induced transitions. The interplay of noise and variability (in several model parameters) could be essential for the dynamics of a biophysical network, because the diverse elements determine the net dynamics, and thus the response of the net to a stochastic forcing.